

# Vacuum Ultraviolet (VUV) Photodecomposition of Urea Isolated in Cryogenic Matrix: First Detection of Isoourea

Fabrice Duvernay, Thierry Chiavassa,\* Fabien Borget, and Jean-Pierre Aycard

Physique des Interactions Ioniques et Moléculaires, UMR 6633, Université de Provence et CNRS, Centre de St Jérôme, case 252, 13397 Marseille Cedex 20, France

Received: April 13, 2005; In Final Form: May 17, 2005

Vacuum ultraviolet (VUV) irradiation at wavelengths of  $\lambda > 160$  nm of urea- $h_4$  ( $\text{NH}_2\text{CONH}_2$ ) and urea- $d_4$  ( $\text{ND}_2\text{COND}_2$ ) has been monitored by Fourier transform infrared spectroscopy in argon and xenon matrixes. Several primary photoproducts, such as  $\text{HNCO}:\text{NH}_3$  (isocyanic acid:ammonia),  $\text{CO}:\text{N}_2\text{H}_4$  (carbon monoxide:hydrazine) molecular complexes, and isourea ( $\text{H}_2\text{N}(\text{OH})\text{C}=\text{NH}$ ), which is reported for the first time, were characterized. The assignment of complexes was achieved by co-depositing the pairs of respective species, whereas the isourea identification was based on the comparison between the experimental and theoretical (B3LYP) infrared spectra. Isourea is found in the argon matrix in its most stable (s-Z)-(E) configuration. It is an intermediate in the VUV decomposition process; its dehydration leads to the  $\text{NH}_2\text{CN}:\text{H}_2\text{O}$  complex. In the xenon matrix, the photochemistry of urea yields the  $\text{HNCO}:\text{NH}_3$  complex as a major product, whereas the  $\text{CO}:\text{N}_2\text{H}_4$  complex is observed in trace amounts. The observed differences between the argon and xenon matrixes suggest the crossing between  $S_1$  and  $T_1$  potential surfaces of urea to be responsible for the formation of the  $\text{HNCO}:\text{NH}_3$  complex. A comparison is also performed with other carboxamides, such as formamide ( $\text{HCONH}_2$ ) or acetamide ( $\text{CH}_3\text{CONH}_2$ ).

## 1. Introduction

Urea ( $\text{NH}_2\text{CONH}_2$ ), isolated by Rouelle in 1773, is the first organic molecule which was synthesized in the laboratory from inorganic precursors in 1828 by Wohler.<sup>1</sup> It was probably abundant on Earth in earlier time periods<sup>2</sup> and could have a role in the formation of prebiotic molecules. For example, amino acids can be formed in the ultraviolet (UV)-irradiated aqueous solution of urea and maleic acid.<sup>3</sup> Similarly, pyrimidine bases can be synthesized in an aqueous solution of cyanoacetylene and urea at 100 °C.<sup>4</sup> Thus, the tentative urea detection by the Infrared Space Observatory (ISO) in the infrared spectra of interstellar ices is interesting, from a biologically point of view, and may help to establish the importance of extraterrestrial sources of organic material on Earth prior to the onset of life.<sup>5</sup> Previous laboratory experiments involving vacuum ultraviolet (VUV) irradiation of  $\text{HNCO}$ , which is an interstellar molecule, in solid samples at 10 K demonstrated that it could be a source of urea in interstellar ices.<sup>5</sup>

In the interstellar medium, under the electromagnetic radiation emanating from stars, molecules are subjected to VUV-induced photochemical processes that occur both in the gas phase and in the solid phase (cold dust grains).<sup>6</sup> Thus, the behavior of urea toward VUV irradiation at low temperature is important for the refinement of interstellar chemistry models and should also improve our understanding of the carboxamide photochemistry. Among carboxamides, acetamide ( $\text{CH}_3\text{CONH}_2$ ) and formamide ( $\text{HCONH}_2$ ) have received some particular attention. The photolysis of acetamide was studied in solutions and in the gas phase; products resulting from dehydration ( $\text{CH}_3\text{CN}$ ) or decarboxylation ( $\text{CH}_3\text{NH}_2$ ) processes were identified.<sup>7,8</sup> Photode-

composition of formamide has been performed at 193 nm in argon and xenon cryogenic matrixes by Lundell et al.<sup>9</sup> Two major reaction channels were indicated, leading to products coming from decarbonylation and dehydrogenation processes. These products— $\text{NH}_3$  and  $\text{HNCO}$ , respectively—were complexed with CO and  $\text{H}_2$  in the same matrix cage where the formamide precursor was located. However, the product of formamide dehydration ( $\text{HCN}$ ) was not observed by Lundell et al. As shown earlier by Bosco et al.,<sup>10</sup> using electron spin resonance spectroscopy, the primary reaction channels of the amide photodissociation reveal the presence of free radicals. High-level ab initio studies have recently been conducted<sup>11,12</sup> to explore the potential energy surfaces of formamide and acetamide photodissociation along the ground-state and low-excited-state pathways. Calculations show that the favorable dissociation pathways exist in (i) the formation of  $\text{H}_2\text{N}$  and CHO radicals in the lowest singlet state ( $S_1$ ), followed by the formation of CO and  $\text{NH}_3$ , and (ii) the formation of  $\text{HNCO}$  and  $\text{H}_2$  through an intersystem crossing from the  $S_1$  to the lowest ( $T_1$ ) triplet state.<sup>11</sup> For acetamide,<sup>12</sup> the same decarbonylation mechanism is observed, in addition to the dehydration process leading to  $\text{CH}_3\text{CN}$ ; the theoretical description involves two steps, in which an intermediate (ethanimidic acid,  $\text{CH}_3\text{C}(\text{OH})=\text{NH}$ ) is produced.

The analysis of the UV spectrum of crystalline urea<sup>13</sup> reveals three bands, in good agreement with theoretical predictions: <sup>14,15</sup> the  $n \rightarrow \pi^*$  transition at 178 nm, the  $\pi \rightarrow \pi^*$  transition at 161 nm, and an additional transition at 156 nm of as-yet unknown origin.<sup>13</sup> Therefore, the use of a VUV source is essential to accomplish the urea photolysis.

The purpose of this work is to study, for the first time, the photoreactivity of urea- $h_4$  and of its urea- $d_4$  isotopomer trapped in low-temperature matrixes (argon and xenon) with a discharge hydrogen flow lamp ( $\lambda > 160$  nm). The advantage of working

\* Author to whom correspondence should be addressed. Telephone: +33 491-288-580. Fax: +33 491-636-510. E-mail address: Thierry.chiavassa@up.univ-mrs.fr.

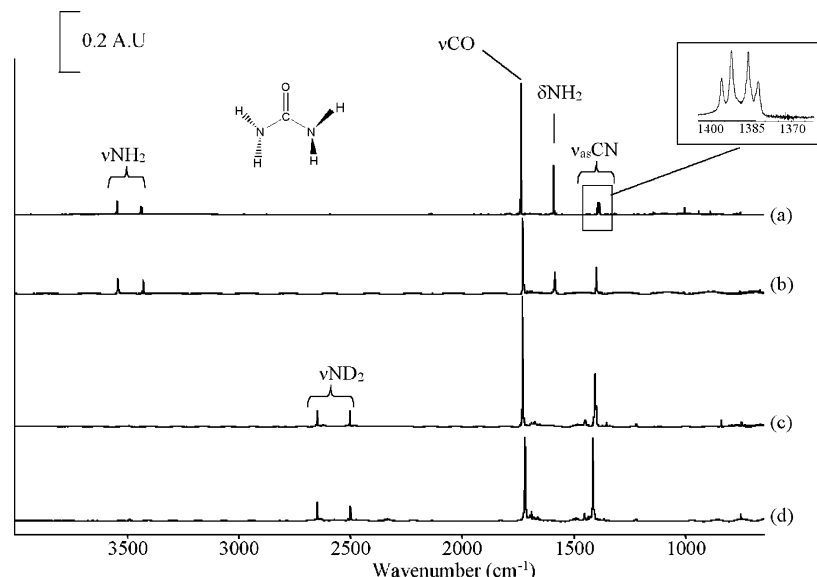


**Figure 1.** Fourier transform infrared (FTIR) spectra of urea- $h_4$  deposited and recorded at 10 K in an argon matrix (spectrum a), urea- $h_4$  deposited and recorded at 10 K in a xenon matrix (spectrum b), urea- $d_4$  deposited at 30 K and recorded at 10 K in an argon matrix (spectrum c), and urea- $d_4$  deposited at 30 K and recorded at 10 K in a xenon matrix (spectrum d). The substructure of argon matrix–urea composite ( $C_2$  symmetry) is shown in the inset.

in a cryogenic matrix, rather than in the gas phase, is first the cage effect, which generally prevents the diffusion of photo-fragments. Thus, the formed species have the same stoichiometry than the precursor. Second, the formed species, which are often very reactive, are stabilized in the low-temperature matrix. A comparison of the urea photoreactivity to that of other carbox-amides (formamide, acetamide) is also presented.

## 2. Experimental Details

Because urea (Aldrich, 99% purity) has a low vapor pressure at room temperature, it was sublimed at 50 °C, placed in a glass oven connected to the cryostat, and entrained by argon (Linde, 99.99% purity) or xenon (Air Liquide, 99.99% purity) toward a gold-plated mirror (cooled to 10 K) with a rate of 0.7 mmol/min, to obtain a rare gas matrix. During the deposition, the cryostat was kept under a constant pressure of  $3.5 \times 10^{-7}$  mbar. A sample annealing at 30 K is very useful to convert kinetic molecular complexes into thermodynamic complexes. This process allows a reliable characterization of products to be obtained. The same experimental conditions were applied in urea- $d_4$  (Eurisotop, 98% purity) experiments.

Argon and xenon matrixes with co-deposited pairs of compounds—namely, HNCO/ $NH_3$ , DNCO/ $ND_3$ , CO/ $N_2H_4$ ,  $NH_2$ -CN/ $H_2O$ , and  $ND_2$ CN/ $D_2O$ —have also been prepared to assist in the identification of UV irradiation products.

Pure isocyanic acid (HNCO) was synthesized using the method described by Herzberg<sup>16</sup> and modified by Sheludya-kov.<sup>17</sup> It was degassed before each deposition. Ammonia was supplied by Air Liquide (N36,  $H_2O < 200$ ). To avoid any reaction between HNCO and  $NH_3$  in the gas phase, prior to the cryogenic trapping,  $NH_3$ /Ar (20/500) and HNCO/Ar (1/500) were deposited by two separate inlets. The concentrations were estimated with standard manometric techniques. The HNCO/Ar mixture can be converted (with a yield of  $>50\%$ ) to DNCO by exchange with  $D_2O$  (Aldrich, 99% purity) adsorbed on the glass walls of the sample preparation and deposition system.<sup>18</sup> DNCO and  $ND_3$  (Air Liquide, 99% purity) co-deposition experiments were made under identical conditions to those applied for HNCO and  $NH_3$ .

**TABLE 1: Assignments of the Vibrational Bands of Urea- $h_4$  and Urea- $d_4$  in Solid Argon and Xenon Deposited and Recorded at 10 K**

assignment <sup>a</sup>	Vibrational Bands ( $cm^{-1}$ )			
	Urea- $h_4$		Urea- $d_4$	
	Ar	Xe	Ar	Xe
$\nu_{as}(NH_2)$	3545	3541	2661	2657
$\nu_{as}(NH_2)$	3544		2648	2650
$\nu_s(NH_2)$	3440	3430	2510	2511
$\nu_s(NH_2)$	3436		2502	2500
$\nu(CO)$	1745	1723	1729	1719
$\delta_{as}(NH_2)$	1590	1585	1115	
$\delta_s(NH_2)$	1590	1586	1221	1222
$\nu_{as}(CN)$	1389	1398	1405	1413
$\rho_s(NH_2)$	1145	1149		
$\rho_{as}(NH_2)$	1004	1008		
$\nu_s(CN)$	940	956	840	847
$\omega(CO)$	754	756	747	753
$\tau(NH_2)$	616			

<sup>a</sup>  $\nu$ , stretching;  $\delta$ , bending;  $\rho$ , rocking,  $\tau$ , torsion; and  $\omega$ , wagging.

The hydrazine sample (Aldrich, 98% purity) was transferred under nitrogen to a distillation apparatus, refluxed over NaOH during 4 h, then distilled;<sup>19</sup> the fraction boiling at 113 °C was collected. Carbon monoxide (Air Liquide, 99.99% purity) and hydrazine gases were mixed at different ratios with argon or xenon in a Pyrex bulb prior to the deposition with a rate of 0.6 mmol/min onto the mirror surface cooled to 10 K (argon) or 30 K (xenon).

Cyanamide (Aldrich, 99% purity) was placed into a glass oven that was connected directly to the cryostat, then entrained at room temperature with a  $H_2O$ /Ar (5/400) mixture onto the mirror cooled to 10 K, with a rate of 0.7 mmol/min. Water was doubly distilled before each use. The cyanamide- $d_2$  sample was prepared by successive exchanges (four times) with  $D_2O$ .<sup>20</sup>

VUV irradiations ( $\lambda > 160$  nm) were performed using a microwave discharge hydrogen flow lamp (Ophos Instruments) mounted directly onto the sample chamber. UV radiation was transmitted to the sample through a  $SiO_2$  window in the wavelength range up to 160 nm. The infrared spectra were recorded in the reflection mode (in fact, double transmission) between 4000 and 600  $cm^{-1}$ , with a Nicolet Magna 750 FTIR

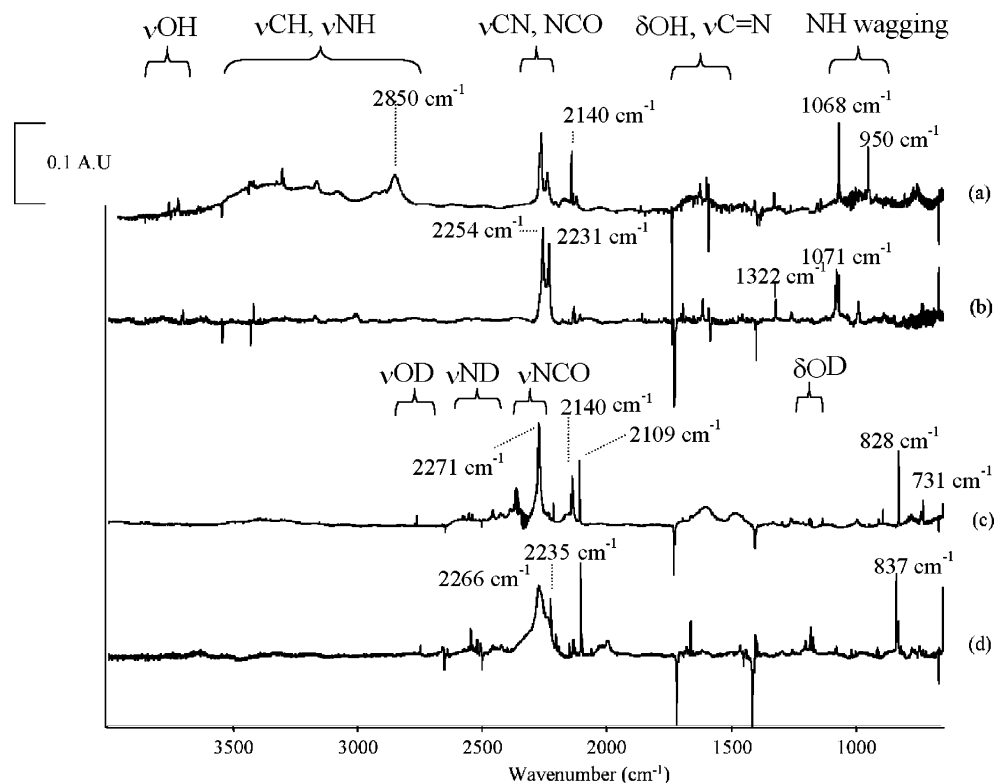


**Figure 2.** Infrared (IR) difference spectra showing the net photolysis effects. Spectra were recorded before irradiation subtraction in each case from urea- $h_4$  at 10 K in argon after 450 min of irradiation ( $\lambda > 160$  nm) (spectrum a), urea- $h_4$  in xenon at 10 K after 200 min of irradiation ( $\lambda > 160$  nm) (spectrum b), urea- $d_4$  in argon at 10 K after 450 min of irradiation ( $\lambda > 160$  nm) (spectrum c), and urea- $d_4$  in xenon at 10 K after 450 min of irradiation ( $\lambda > 160$  nm) (spectrum d). The bands of urea and those due to new products appear as negative and positive, respectively.

spectrometer that is equipped with a liquid  $N_2$  cooled detector, a germanium-coated KBr beamsplitter, and a globar source. One hundred interferograms were collected for each spectrum, and the resolution was set to  $0.12\text{ cm}^{-1}$ .

### 3. Computational Details

Calculations were performed with the Gaussian 98 package<sup>21</sup> at the B3LYP/6-311+G(2d,2p) level, which is known to supply reliable predictions of vibrational frequencies. Four stereoisomers of isourea have been taken into account: (s-Z)–(E), (s-Z)–(Z), (s-E)–(Z), and (s-E)–(E). The first component of this notation indicates the rotation about the C–O bond, the second describes the configuration at the C=N double bond. All four structures have been fully optimized, and then their harmonic vibrational frequencies and absolute IR intensities were computed. The calculated frequencies were overestimated, with respect to the experimental values; therefore, they have been scaled by a standard factor of 0.96 (0.97 in the case of isourea- $d_4$ ).

### 4. Results

**4.1. Fourier Transform Infrared Spectra of Urea in Rare-Gas Matrixes.** Experimental studies on the urea molecule in the gas phase<sup>24</sup> or isolated in a rare gas matrix<sup>25,26</sup> suggest, for this molecule, a nonplanar structure with the  $C_2$  rather than  $C_{2v}$  symmetry. In the solid state, neutron diffraction experiments revealed the existence of a planar urea structure.<sup>27–29</sup> This planar conformation in the solid state was also determined by numerous theoretical calculations.<sup>30,31</sup> The Fourier transform infrared (FTIR) spectra of urea- $h_4$  and its urea- $d_4$  isotopomer in argon and, for the first time, in xenon matrixes are displayed in Figure 1; respective experimental frequencies and assignments of bands are collected in Table 1. Our spectra in argon matrixes are in

good agreement with those reported in previous studies,<sup>25,26,32</sup> and they show that urea is isolated in its monomeric form. The Ar-to-Xe matrix shifts were small, which allowed us to assign the bands observed in the xenon matrix on the basis of those already assigned in argon matrixes. The most intense band, in both Ar and Xe, is the  $\nu(\text{C}=\text{O})$  stretching mode, which is located at  $1745\text{ cm}^{-1}$  and  $1723\text{ cm}^{-1}$ , respectively ( $1729$  and  $1719\text{ cm}^{-1}$  in the case of urea- $d_4$ ). Other strong absorptions at  $3500$ ,  $1590$ , and  $1389\text{ cm}^{-1}$  (in argon) are assigned, respectively, to  $\nu(\text{NH}_2)$ ,  $\delta(\text{NH}_2)$ , and  $\nu_{\text{as}}(\text{CN})$  modes. One of the most striking features is the presence of four bands observed for the  $\nu_{\text{as}}(\text{CN})$  mode of urea- $h_4$  isolated in the argon matrix (see Figure 1). This multiplet disappears completely for the deuterated molecule or in a xenon matrix. As underlined by Dobrowolski et al.,<sup>32</sup> a Fermi resonance coupling of the  $\nu_{\text{as}}(\text{CN})$  mode and the  $\nu_{\text{s}}(\text{CN}) + \omega_{\text{s}}(\text{NH}_2)$  combination mode could explain this feature.

**4.2. Photochemistry of Urea- $h_4$  and Urea- $d_4$ .** The VUV irradiations ( $\lambda > 160$  nm) of urea- $h_4$  and urea- $d_4$  were performed for several hours in argon and xenon matrixes at 10 K. The half-life time of urea- $h_4$  and urea- $d_4$  decomposition in argon is reached after 45 and 60 min, whereas 90% of urea is consumed after 330 and 450 min, respectively. In xenon, the half-life times of urea- $h_4$  and urea- $d_4$  are 40 and 90 min, respectively; 90% of urea- $h_4$  is decomposed after 200 min. The complexity of the infrared spectra obtained after a quasi-complete destruction of the precursor molecule suggests the presence of several photoproducts. New vibrational features (showed as positive bands in Figure 2 and listed in Table 2) are observed in the typical regions of water absorptions ( $3700$ – $3600\text{ cm}^{-1}$  and  $1650$ – $1580\text{ cm}^{-1}$ ), cyanamide ( $\text{NH}_2\text{CN}$ ) or isocyanic acid ( $\text{HNCO}$ ) ( $2280$ – $2200\text{ cm}^{-1}$ ), carbon monoxide ( $2160$ – $2130\text{ cm}^{-1}$ ), hydrazine ( $\text{N}_2\text{H}_4$ ), and ammonia ( $\text{NH}_3$ ); the latter is observed especially well, because of intense NH wagging or inversion modes

**TABLE 2: Assignments of the Vibrational Bands Observed after 450 min of VUV Irradiation of Urea-h<sub>4</sub> in Argon and Xenon Matrices at 10 K before and after Annealing**

Vibrational Bands for Urea-h <sub>4</sub> (cm <sup>-1</sup> ) <sup>a</sup>				species	assignment <sup>b</sup>
Ar		Xe			
10 K	10 K after 30 K	10 K	10 K after 30 K		
<b>3718</b>	<b>3718</b>	<b>3700</b>	<b>3700</b>	H <sub>2</sub> O (+ NH <sub>2</sub> CN)	$\nu(\text{OH})$
		3479	3479	HNCO	$\nu(\text{NH})$
<b>3298</b>	<b>3312</b>			HCN (+ NH <sub>2</sub> OH)	$\nu(\text{CH})$
<b>3163</b>	<b>3163</b>			NH <sub>2</sub> OH (+ HCN)	$\nu(\text{OH})$
2850	2850			HNCO(+ NH <sub>3</sub> )	$\nu(\text{NH})$
<b>2797</b>	<b>2797</b>			H <sub>2</sub> CO	$\nu(\text{CH})$
<b>2792</b>	<b>2792</b>			H <sub>2</sub> CO (+ N <sub>2</sub> H <sub>2</sub> )	$\nu(\text{CH})$
2264	2268	2268	2268	HNCO(+ NH <sub>3</sub> )	$\nu_{\text{as}}(\text{NCO})$
2259	2259	2254	2254	HNCO	$\nu_{\text{as}}(\text{NCO})$
<b>2258</b>	<b>2258</b>	<b>2257</b>	<b>2257</b>	NH <sub>2</sub> CN (+ H <sub>2</sub> O)	$\nu(\text{CN})$
2238	2243	2231	2231	HNCO (+ NH <sub>3</sub> ) <sub>2</sub>	$\nu_{\text{as}}(\text{NCO})$
2140	2139–2138–2137			CO (+ N <sub>2</sub> H <sub>4</sub> )	$\nu(\text{CO})$
2138		2133	2133	CO	$\nu(\text{CO})$
1863	1863	1858	1858	HCO	$\nu(\text{CO})$
<b>1742</b>	<b>1742</b>			H <sub>2</sub> CO	$\nu(\text{CO})$
<b>1741</b>	<b>1741</b>			H <sub>2</sub> CO (+ N <sub>2</sub> H <sub>2</sub> )	$\nu(\text{CO})$
1697	1697	1694	1694	isourea <sup>c</sup>	$\nu(\text{C}=\text{N})$
<b>1598</b>	<b>1598</b>	<b>1588</b>	<b>1588</b>	H <sub>2</sub> O (+ NH <sub>2</sub> CN)	$\delta(\text{OH})$
1326	1330	1322	1322	HNCO (+ NH <sub>3</sub> )	$\nu_{\text{s}}(\text{NCO})$
<b>1315</b>				N <sub>2</sub> H <sub>2</sub> (+ H <sub>2</sub> CO)	
1068	1069–1065	1071	1069	NH <sub>3</sub> (+ HNCO)	$\omega(\text{NH})$
950	958			N <sub>2</sub> H <sub>4</sub> (+ CO)	$\omega(\text{NH})$

<sup>a</sup> The bands appearing in bold typeface are due to products of secondary photochemical processes. <sup>b</sup>  $\nu$ : stretching;  $\delta$ : bending;  $\rho$ : rocking;  $\tau$ : torsion; and  $\omega$ : wagging. <sup>c</sup> After 450 min of VUV irradiation of urea-h<sub>4</sub> in an argon matrix (200 min in a xenon matrix), only the most intense band of isourea is visible, because it undergoes a secondary photochemical process.

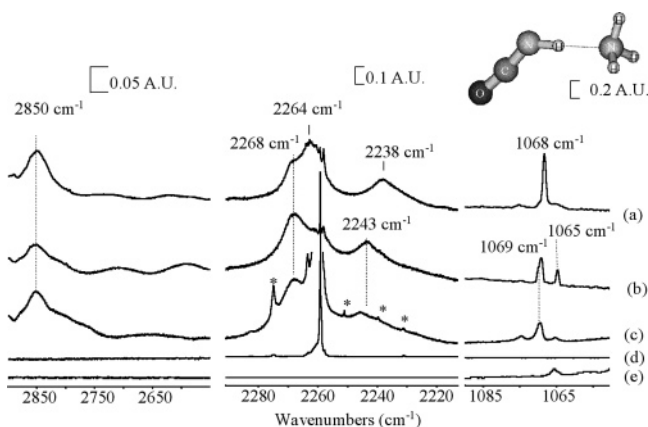


**Figure 3.** FTIR spectra of urea in an argon matrix at 10 K after 450 min of irradiation ( $\lambda > 160$  nm) (spectrum a), after annealing at 30 K (spectrum b), HNCO/Ar and NH<sub>3</sub>/Ar co-deposition experiment at 10 K (spectrum c) (where the asterisk symbol “\*” denotes rotational bands of monomeric HNCO isolated in an argon matrix<sup>35</sup>) (spectrum c), HNCO/Ar 1/1000 at 10 K (spectrum d), and NH<sub>3</sub>/Ar 1/1000 at 10 K (the feature at 1065 cm<sup>-1</sup> is due to the NH<sub>3</sub> aggregate) (spectrum e). Dotted lines label the band related to the complex HNCO:NH<sub>3</sub>.

(1100–940 cm<sup>-1</sup>). Most of these new bands are shifted in frequency, with respect to the values determined for the isolated monomeric species in argon or xenon matrices. This is to be expected when a molecular complex is formed during the photolysis from a single precursor within the given matrix cage. Indeed, hot fragments cannot escape from the cage, and what follows is that the created molecular complexes have the stoichiometry (CH<sub>4</sub>N<sub>2</sub>O) of the precursor.

**4.3. Formation of HNCO:NH<sub>3</sub> Complex.** The VUV irradiation (10 K) of urea-h<sub>4</sub> in the argon matrix leads to the bands at 2850, 2264, 2238, 1326, and 1068 cm<sup>-1</sup> (Figure 3a), which all exhibit similar evolution patterns during the irradiation process. The locations of these bands are similar to those expected for the HNCO:NH<sub>3</sub> complex<sup>33</sup> (see Figure 3c). The assignments

become obvious when the spectrum recorded after the annealing at 30 K (Figure 3b) is compared with the spectrum of a HNCO/NH<sub>3</sub>/Ar mixture (Figure 3c). Indeed, the band at 2264 cm<sup>-1</sup> decreased after the annealing, whereas the feature located at 2268 cm<sup>-1</sup> increased. The bands at 2238 and 1326 cm<sup>-1</sup> are shifted to 2243 and 1330 cm<sup>-1</sup>, respectively (see Figure 3b, Table 2). In the typical region of the NH<sub>3</sub> inversion mode, the band at 1068 cm<sup>-1</sup> disappeared, being replaced by two bands at 1069 and 1065 cm<sup>-1</sup>. These changes can be understood in term of transition from a high-energy HNCO:NH<sub>3</sub> complex (kinetic complex formed at 10 K) to a lowest-energy HNCO:NH<sub>3</sub> complex (thermodynamic complex established at 30 K).

In a previous study,<sup>33</sup> we reported, in detail, on the assignment of these bands to the HNCO:NH<sub>3</sub> complex. Thus, the intense band at 2268 cm<sup>-1</sup> and the weaker band at 1330 cm<sup>-1</sup> are due to the  $\nu(\text{OCN})$  antisymmetric and symmetric stretching modes of HNCO, respectively. The absorption at 1069 cm<sup>-1</sup> is due to the inversion mode of complexed ammonia, whereas the feature at 2850 cm<sup>-1</sup> is related to the NH stretching mode of complexed HNCO. A strong downshift is observed, in comparison with the HNCO monomer value (3512 cm<sup>-1</sup>), and suggests the existence of a 1:1 hydrogen-bonded complex, with HNCO bound via its H atom to the NH<sub>3</sub> nitrogen. The geometry of the complex, established with the aid of previous calculations,<sup>33</sup> is recalled in Figure 3. The band at 2243 cm<sup>-1</sup> has been tentatively assigned to the HNCO:(NH<sub>3</sub>)<sub>2</sub> complex,<sup>33</sup> in view of its sensitivity to the NH<sub>3</sub> concentration in the mixture. Moreover, it becomes more intense upon the increase of the sample temperature, in parallel to the easier diffusion of NH<sub>3</sub> in the matrix.<sup>33</sup> The absorption at 1065 cm<sup>-1</sup> evolves identically as the 2243 cm<sup>-1</sup> feature, and is located in the frequency range of ammonia aggregates.<sup>34</sup> Thus, it can probably also be assigned to HNCO:(NH<sub>3</sub>)<sub>2</sub>.

In the  $\nu(\text{CN})$  and  $\nu(\text{NCO})$  region (2280–2250 cm<sup>-1</sup>), two narrow bands, which are located at 2259 and 2258 cm<sup>-1</sup>, appeared after the irradiation. The frequencies of these bands



**TABLE 3: Assignments of the Vibrational Bands Observed after 450 min of VUV Irradiation of Urea-d<sub>4</sub> in an Argon Matrix and a Xenon Matrix at 10 K before and after Annealing**

Vibrational Bands for Urea-d <sub>4</sub> (cm <sup>-1</sup> ) <sup>a</sup>				species	assignment <sup>b</sup>
Ar		Xe			
10 K	10 K after 30 K	10 K	10 K after 30 K		
2769	2769			D <sub>2</sub> O	$\nu(\text{OD})$
<b>2761</b>	<b>2761</b>	<b>2747</b>		D <sub>2</sub> O (+ ND <sub>2</sub> CN)	$\nu(\text{OD})$
2654	2654	2660		isourea-d <sub>4</sub>	$\nu(\text{OD})$
<b>2575</b>	<b>2575</b>			ND <sub>2</sub> CN (+ D <sub>2</sub> O)	$\nu(\text{ND})$
<b>2535</b>	<b>2535</b>			DNCND (+ D <sub>2</sub> O)	$\nu(\text{ND})$
2457	2457			?	
2415	2415			D <sub>2</sub> O (+?)/ND <sub>3</sub> (+?)	$\nu(\text{OD}), \nu(\text{ND})$
2284	2284			DOCN	$\nu(\text{OCN})$
2271	2290–2259	2266	2274	DNCO (+ ND <sub>3</sub> )	$\nu(\text{NCO})$
<b>2258</b>	<b>2258</b>	<b>2258</b>	<b>2258</b>	ND <sub>2</sub> CN (+ D <sub>2</sub> O)	$\nu(\text{CN})$
		2227	2227	DNCO	$\nu(\text{NCO})$
2214	2214			D <sub>2</sub> NNCO	$\nu(\text{NCO})$
2151	2151	2136		CO (+?)	$\nu(\text{CO})$
2145	2145	2126		CO (+?)	$\nu(\text{CO})$
2143	2143			CO (+ ND <sub>3</sub> )	$\nu(\text{CO})$
2140	2139–2138–2137			CO (+ N <sub>2</sub> D <sub>4</sub> )	$\nu(\text{CO})$
2138		2133	2133	CO	$\nu(\text{CO})$
<b>2109</b>	<b>2106</b>	<b>2105</b>	<b>2105</b>	DNCND (+ D <sub>2</sub> O)	$\nu(\text{NCN})$
<b>2066</b>				D <sub>2</sub> CO (+ N <sub>2</sub> D <sub>2</sub> )	$\nu(\text{CD})$
1662	1662	1662	1662	isourea-d <sub>4</sub>	$\nu(\text{C=N})$
1405	1405	1405	1405	(+?)	
1399	1399	1399	1399	(+?)	
<b>1180</b>	<b>1180</b>	<b>1182</b>	<b>1182</b>	ND <sub>2</sub> CN (+ D <sub>2</sub> O)	$\delta(\text{OD})$
828	830–826	837	829	ND <sub>3</sub> (+ DNCO)	$\omega(\text{NH})$
731				N <sub>2</sub> D <sub>4</sub> (+ CO)	$\omega(\text{NH})$

<sup>a</sup> The bands denoted by bold typeface are due to products of secondary photochemical processes. <sup>b</sup>  $\nu$ , stretching;  $\delta$ , bending;  $\rho$ , rocking;  $\tau$ , torsion; and  $\omega$ , wagging.

were not altered by the annealing effect. The former is due to HNCO monomer.<sup>35</sup> The amount of this species formed in the present experiment is very small, which explains why we could not observe the rotational bands related to HNCO in the argon matrix (see Figure 3a). The second band is due to another species, which will be discussed below.

The spectrum analysis of the urea-d<sub>4</sub> isotopomer in the argon matrix irradiated at 10 K leads to the appearance of bands at 828 and 2271 cm<sup>-1</sup> (see Figure 2c, Table 3). After annealing at 30 K, the band at 2271 cm<sup>-1</sup> disappears, while two broad bands, at 2290 and 2259 cm<sup>-1</sup>, increase their intensities (see Table 3). At the same time, the band at 828 cm<sup>-1</sup> disappears, while two sharp bands, at 830 and 826 cm<sup>-1</sup>, grow. This compartment is similar to that which we have already mentioned for the HNCO:NH<sub>3</sub> complex. We can thus assign the bands at 2290 and 830 cm<sup>-1</sup> to the DNCO:ND<sub>3</sub> complex. The band at 2290 cm<sup>-1</sup> is due to the  $\nu(\text{OCN})$  antisymmetric-stretching mode of the complex and it is strongly shifted (+50 cm<sup>-1</sup>), with respect to the DNCO monomer value<sup>18</sup> (2235 cm<sup>-1</sup>). The band at 830 cm<sup>-1</sup> is due to the ND<sub>3</sub> inversion mode (see Table 3). Finally, the bands located after annealing at 2259 and 826 cm<sup>-1</sup> can be assigned to DNCO:(ND<sub>3</sub>)<sub>2</sub>.

In the xenon matrix, we observe that the photodecomposition of urea-h<sub>4</sub> (urea-d<sub>4</sub>) leads preferentially to the formation of the HNCO:NH<sub>3</sub> (DNCO:ND<sub>3</sub>) complex (see Figure 2b, 2d). Spectra are dominated by the set of bands at 2268, 2231, 1322, and 1071 cm<sup>-1</sup> (2266, 837 cm<sup>-1</sup> for urea-d<sub>4</sub>), with frequencies similar to their argon matrix analogues. These are collected in Table 2 (Table 3 in the case of urea-d<sub>4</sub>), with their respective assignments. In addition, we observe the formation of the HNCO monomer, as it is shown by the emergence of bands at 3479 and 2254 cm<sup>-1</sup> (2226 cm<sup>-1</sup> for DNCO). It is noticeable that, in the xenon matrix, the efficiency of isolated HNCO production is higher than that in argon (where HNCO is formed in trace quantities).

**4.4. Formation of the CO:N<sub>2</sub>H<sub>4</sub> Complex.** In a previous study,<sup>36</sup> the geometries, energies, and vibrational properties of CO:N<sub>2</sub>H<sub>4</sub> complexes were experimentally investigated using FTIR spectroscopy associated with a computational study.

UV irradiation of urea-h<sub>4</sub> in an argon matrix at 10 K also leads to the decarbonylation process and, consequently, to the formation of CO and N<sub>2</sub>H<sub>4</sub> trapped within the same matrix cage. The two species interact, eventually resulting in the formation of a molecular complex. In the antisymmetric wagging ( $\nu_{12}$  mode) region of the N<sub>2</sub>H<sub>4</sub> spectrum, a strong band appears at 950 cm<sup>-1</sup> (see Figure 2a). This latter band is slightly downshifted, with respect to the monomer value<sup>37</sup> (953 cm<sup>-1</sup>). In the CO stretching region (Figure 2a), an intense band appears at 2140 cm<sup>-1</sup>, slightly upshifted from the monomer value in an argon matrix<sup>38</sup> (2138 cm<sup>-1</sup>). Just as in the case of the HNCO:NH<sub>3</sub> complex after the matrix annealing at 30 K, important changes appear in the spectrum of irradiated urea.<sup>36</sup> The band located at 2140 cm<sup>-1</sup> disappears, whereas new bands at 2139, 2138, and 2137 cm<sup>-1</sup> grow. At the same time, in the  $\nu_{12}$  region, the band at 950 cm<sup>-1</sup> disappears at the expense of a band at 958 cm<sup>-1</sup>. The spectrum obtained after annealing is thus similar to that resulting from the CO/N<sub>2</sub>H<sub>4</sub>/Ar mixture, with N<sub>2</sub>H<sub>4</sub> being in excess.<sup>31</sup> All these new bands are related to three different structures of CO:N<sub>2</sub>H<sub>4</sub> complexes.

UV irradiation of the urea-d<sub>4</sub> isotopomer in an argon matrix at 10 K also leads to the formation of the CO:N<sub>2</sub>D<sub>4</sub> complex, which is characterized by a band at 2140 cm<sup>-1</sup>, because of complexed CO (see Figure 2c, Table 3). Another band at 731 cm<sup>-1</sup> that is related to the  $\nu_{12}$  mode of hydrazine-d<sub>4</sub> is 2 cm<sup>-1</sup> downshifted, with respect to the monomer frequency<sup>37</sup> (see Figure 2c, Table 3), confirming the previous experimental results for the CO:N<sub>2</sub>H<sub>4</sub> complex, which gave a 3 cm<sup>-1</sup> shift.

In a xenon matrix, CO is detected as a trace product during the photodecomposition of urea-h<sub>4</sub> (urea-d<sub>4</sub>), as shown by the

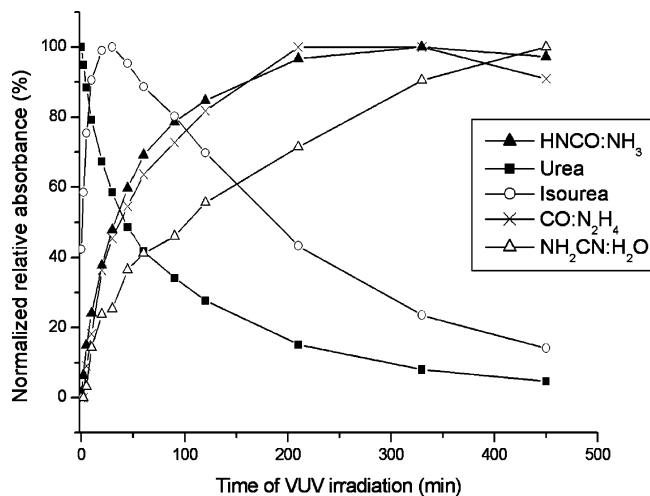


**Figure 4.** Kinetic evolution of products during the photolysis of urea- $h_4$  (wavelength of  $\lambda > 160$  nm) in an argon matrix at 10 K. Normalized integrated absorbances of characteristic bands are plotted versus irradiation time.

weak absorption at  $2133\text{ cm}^{-1}$  (see Figure 2b, 2d), which is typical of the CO monomer.<sup>38</sup> Two smaller sidebands at  $2136$  and  $2126\text{ cm}^{-1}$  could also be assigned to complexed CO, but neither  $\text{N}_2\text{H}_4$  nor  $\text{N}_2\text{D}_4$  were detected.

In summary to this part of the study,  $\text{CO:N}_2\text{H}_4$  and  $\text{HNCO:NH}_3$  complexes are the two major primary products of the VUV urea irradiation in argon matrixes ( $\text{CO:N}_2\text{D}_4$  and  $\text{DNCO:ND}_3$  in the case of urea- $d_4$ ). Kinetic curves depicting the evolution of these products under irradiation are reported in Figure 4. In the xenon matrix, the major product is the  $\text{HNCO:NH}_3$  ( $\text{DNCO:ND}_3$  for urea- $d_4$ ) complex. However, these two species do not allow for a description of the entire spectrum obtained after the photolysis of urea- $h_4$  or urea- $d_4$ . In particular several new bands emerge in the water absorption region. Our attention will be now focused on another primary product, which is rapidly formed and consumed and has a key role in the involved photochemistry: the isourea, which is a tautomer of urea.

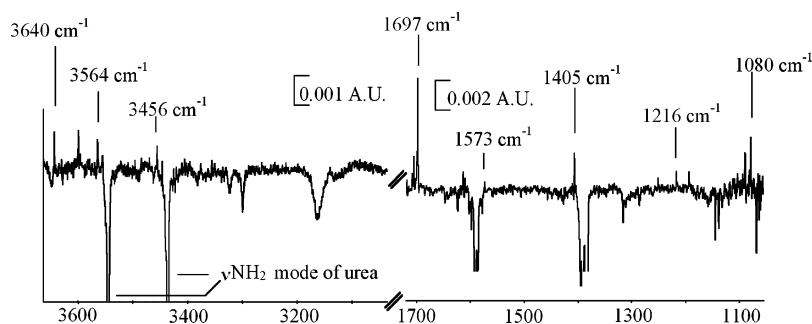
**4.5. Isourea Formation.** Upon irradiation of urea- $h_4$  ( $\lambda > 160$  nm) in an argon matrix, several sharp bands, located at  $3640, 3564, 3456, 1697, 1573, 1405, 1216, 1080, 739, 690\text{ cm}^{-1}$  (Figure 5), grow and reach their maximum intensity after ca. 60 min (see Figure 4). These bands are clearly observed as positive in the difference spectrum (B-A-C) obtained by combining the spectra (A, B, C) obtained for three different irradiation times (0, 60, and 450 min, respectively). Features due to other products ( $\text{HNCO:NH}_3$  and  $\text{CO:N}_2\text{H}_4$ ) and the parent urea appear here as negative. After 450 min of irradiation, only the most intense band of the new species—the one at  $1697\text{ cm}^{-1}$ —is still observed (see Table 2). The position of the bands

cited above and their sharpness are consistent with the formation of an isolated molecule bearing OH ( $3640\text{ cm}^{-1}$ ),  $\text{NH}_2$  ( $3564, 3456\text{ cm}^{-1}$ ), and  $\text{C=N}$  ( $1697\text{ cm}^{-1}$ ) groups. These frequencies are close to those observed for formimidic acid<sup>39</sup> [ $\text{H}(\text{HO})\text{C=NH}$ ], which appear during the 248 nm irradiation of formamide in an argon matrix. In particular, formimidic acid is characterized by an intense band at  $1670\text{ cm}^{-1}$  that is related to the  $\nu(\text{C=N})$  stretching mode.<sup>39</sup> In the same way, urea could be photoisomerized into its tautomer called isourea [ $\text{H}_2\text{N}(\text{HO})\text{C=NH}$ ], which, to date, has never been characterized. However, Piasek et al., in their investigation of the infrared spectra of urea dissolved in polar solvents, have tentatively assigned the  $\nu(\text{C=N})$  of isourea at  $1650\text{ cm}^{-1}$ .<sup>40</sup>

The four possible structures of isourea, fully optimized using the B3LYP method with a 6-311+G(2d,2p) basis set, are reported in Table 4, which lists the respective geometrical parameters and relative energies. According to the calculations, the (s-Z)-(E) stereoisomer is the most stable. Species (s-Z)-(Z), (s-E)-(Z), and (s-E)-(E) stereoisomers are more energetic, by 8.5, 14, and 31 kJ/mol, respectively. The two lowest energy forms—the (s-Z)-(E) and (s-Z)-(Z) isomers—show a quasi-planar arrangement of the  $\text{N}_1\text{COH}_1$  fragment, whereas the (s-E)-(Z) and (s-E)-(E) isomers protrude from the planarity by ca.  $23^\circ$  (see Table 4). In all these structures, just as observed for urea, the  $\text{NH}_2$  group is pyramidal, and the lone electron pair of nitrogen is not involved in the conjugated  $\pi$  system of the  $\text{N}_1\text{COH}_1$  group.

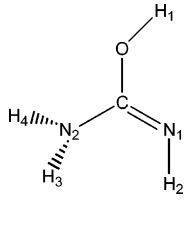
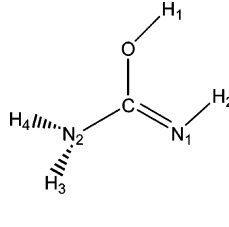
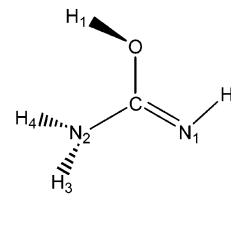
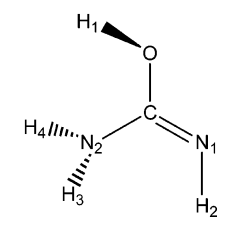
Our elucidation of isourea structures is based on the comparison of experimental infrared frequencies with theoretical values. The harmonic frequencies predicted for each stereoisomer were scaled with a standard factor of 0.96 (Table 5). The four stereoisomers were discerned with the  $\nu(\text{NH}_2)$  and  $\nu(\text{OH})$  stretching frequencies. The  $\nu_{\text{as}}(\text{NH}_2)$  and  $\nu_{\text{s}}(\text{NH}_2)$  stretching modes for the (s-Z)-(E) and (s-Z)-(Z) structures are predicted at  $3557\text{--}3449\text{ cm}^{-1}$  and  $3569\text{--}3460\text{ cm}^{-1}$ , respectively (see Table 5). These predicted values are similar to those experimentally observed for the  $\nu_{\text{as}}(\text{NH}_2)$  and  $\nu_{\text{s}}(\text{NH}_2)$  modes of urea ( $3564\text{--}3456\text{ cm}^{-1}$ ). In the (s-Z)-(E) and (s-Z)-(Z) configurations, there are no intramolecular interactions (hydrogen bond) between the OH and  $\text{NH}_2$  groups, contrary to the two other forms ((s-E)-(Z) and (s-E)-(E)). In the (s-E)-(Z) and (s-E)-(E) isomers, the existence of an intramolecular interaction causes a downshift of ca.  $50\text{ cm}^{-1}$  for  $\nu(\text{NH}_2)$  stretching modes (see Table 5), with respect to the values calculated for the (s-Z)-(E) and (s-Z)-(Z) species.

Weak bands located at  $3564$  and  $3456\text{ cm}^{-1}$  are experimentally found in the vicinity of the urea  $\nu(\text{NH}_2)$  stretching mode (see Figure 5). The isourea (s-E)-(Z) and (s-E)-(E) forms can thus be rejected. In addition, the  $\nu(\text{OH})$  stretching mode is predicted at  $3647$  and  $3693\text{ cm}^{-1}$  for (s-Z)-(E) and (s-Z)-(Z)



**Figure 5.** Difference spectrum (60 min-0 min-450 min) obtained for irradiated urea- $h_4$  in an argon matrix at 10 K. The bands appearing as positive are due to isourea and reach their maximal intensities after ca. 60 min of irradiation. Urea and the other product bands appear as negative.

**TABLE 4: Theoretical Geometrical Parameters of the Four Isourea Stereoisomers**

				
parameter	(s-Z)-(E)	(s-Z)-(Z)	(s-E)-(Z)	(s-E)-(E)
bond lengths (Å)				
$R(\text{OH}_1)$	0.96	0.96	0.96	0.96
$R(\text{CO})$	1.35	1.37	1.37	1.36
$R(\text{CN}_1)$	1.27	1.27	1.26	1.26
$R(\text{CN}_2)$	1.37	1.37	1.39	1.4
$R(\text{NH}_3)$	1	1	1	1.01
$R(\text{NH}_2)$	1.01	1.01	1.01	1.01
$R(\text{H}_1\text{N}_2)$	3.05	3.06	2.3	2.3
$R(\text{H}_1\text{N}_1)$	2.26	2.37	3.06	3.01
$R(\text{H}_4\text{O})$	2.34	2.36	2.53	2.5
$R(\text{H}_2\text{O})$	3.26	2.5	2.39	3.13
bond angles (deg)				
$\alpha(\text{CN}_1\text{H}_2)$	112.8	113	110.9	111.8
$\alpha(\text{COH}_1)$	105.9	108.7	109.6	109.5
$\Theta(\text{N}_1\text{COH}_1)$	1.44	1.34	157.3	154.9
$\Theta(\text{N}_2\text{CN}_1\text{H}_2)$	0	180	180	0
energy (hartree)	-225.3316	-225.3284	-225.3262	-225.3197
$E_{\text{relative}}$ (kJ/mol)	0	8.5	14	31

**TABLE 5: Comparison of Calculated Infrared Spectra for the Four Conformers of Isourea- $h_4$  with the Experimental Frequencies Appearing after 60 min of VUV Irradiation ( $\lambda > 160$  nm) in an Argon Matrix and 40 min in a Xenon Matrix**

assignment <sup>c</sup>	Experimental Frequencies <sup>a</sup> (cm <sup>-1</sup> )		Scaled Frequencies, Using B3LYP/6-311+G(2d,2p) <sup>b</sup> (cm <sup>-1</sup> )			
	argon	xenon	(s-Z)-(E)	(s-Z)-(Z)	(s-E)-(Z)	(s-E)-(E)
$\nu(\text{OH})$	3640 (w)		3647 (16)	3693 (13)	3651 (13)	3671 (16)
$\nu_{\text{as}}(\text{NH}_2)$	3564 (w)		3557 (8)	3569 (10)	3501 (8)	3503 (6)
$\nu_{\text{s}}(\text{NH}_2)$	3456 (vw)		3449 (6)	3460 (8)	3409 (5)	3407 (3)
$\nu(\text{NH})$			3400 (2)	3395 (2)	3391 (4)	3394 (3)
$\nu(\text{C}=\text{N})^d$	1697 (s)	1694	1663 (100)	1673 (100)	1694 (100)	1684 (100)
$\delta(\text{NH}_2)$	1573 (w)		1578 (15)	1560 (16)	1575 (14)	1583 (15)
$\delta(\text{OH}) + \delta(\text{NH})$	1405 (m)		1405 (21)	1380 (23)	1348 (76)	1350 (68)
$\delta(\text{OH})$	1216 (vw)		1217 (23)	1179 (28)	1191 (18)	1206 (31)
$\rho(\text{NH}_2) + \rho(\text{NH})$	1080 (m)	1087	1071 (7)	1078 (25)	1125 (7)	1083 (5)
$\rho(\text{NH}_2) + \rho(\text{NH})$			1047 (34)	1060 (20)	1054 (19)	1046 (36)
$\nu(\text{C}-\text{N}) + \nu(\text{C}-\text{O})$			917 (7)	897 (12)	887 (16)	901 (12)
$\tau(\text{NH})$	739 (w)		728 (7)	714 (20)	802 (7)	778 (40)
$\omega(\text{CNO})$	690 (w)		705 (7)	687 (3)	736 (41)	692 (12)
$\delta(\text{CNO})$			535 (9)	535 (12)	602 (42)	588 (37)
$\tau(\text{OH})$			518 (15)	499 (15)	521 (5)	550 (3)
$\delta(\text{CNO})$			483 (22)	486 (40)	482 (4)	487 (3)
$w(\text{NH}_2)$			461 (36)	418 (12)	398 (39)	374 (33)
$\tau(\text{NH}_2)$			335 (8)	282 (10)	362 (13)	335 (10)
$E_{\text{relative}}$ (kJ/mol)			0	8.5	14	31

<sup>a</sup> Intensity of signal: s, strong; m, medium; and w, weak. <sup>b</sup> Calculated frequencies are scaled by a standard factor of 0.96. Normalized IR intensities are given in parentheses. <sup>c</sup>  $\nu$ , stretching;  $\delta$ , bending;  $\rho$ , rocking;  $\tau$ , torsion; and  $\omega$ , wagging. <sup>d</sup> The absolute calculated intensity (km/mol) of the  $\nu(\text{C}=\text{N})$  modes are as follows: of the (s-Z)-(E) isomer, 480; of the (s-Z)-(Z) isomer, 467; of the (s-E)-(Z) isomer, 358; and of the (s-E)-(E) isomer, 346.

isomers, respectively, whereas the experimental frequency is 3640 cm<sup>-1</sup>. Consequently, VUV irradiation of urea leads to isourea in the (s-Z)-(E) form. It is confirmed also by the excellent agreement observed between the other experimental bands and the calculated infrared spectrum of this stereoisomer (see Table 5). In the same way, we checked that irradiated urea- $d_4$  leads to the formation of isourea- $d_4$  with the (s-Z)-(E) structure (Table 6).

In xenon matrixes, the isourea- $h_4$  (isourea- $d_4$ ) formation is again observed and the UV photoprocess seems to be faster than that in argon matrixes. Isourea reaches its maximal concentration after ca. 40 min. However, only two bands, located

at 1694 and 1087 cm<sup>-1</sup>, could be observed (2660, 1662 cm<sup>-1</sup> for the urea- $d_4$  stereoisomer) (see Table 4 and Table 6) and, consequently, we could not determine the exact structure of isourea in solid xenon.

**4.6. Products of Secondary Photochemical Processes.** After the assignment of vibrational bands to the HNCN:NH<sub>3</sub> and CO: N<sub>2</sub>H<sub>4</sub> complexes and the isourea molecule, some IR absorptions were still not identified. These bands, which appear during the urea photolysis, are reported in Tables 2 and 3 in bold type and belong to products issued from secondary photochemical processes.

**TABLE 6: Comparison of Calculated Infrared Spectra for the Four Conformers of Isoarea-d<sub>4</sub> with the Experimental Frequencies Appearing after 60 min of VUV Irradiation ( $\lambda > 160$  nm)**

assignment <sup>c</sup>	Experimental Frequencies <sup>a</sup> (cm <sup>-1</sup> )		Scaled Frequencies, Using B3LYP/6-311+G(2d,2p) <sup>b</sup> (cm <sup>-1</sup> )			
	argon	xenon	(s-Z)-(E)	(s-Z)-(Z)	(s-E)-(Z)	(s-E)-(E)
$\nu(\text{OD})$	2690 (w)		2681 (9)	2717 (8)	2685 (7)	2700 (9)
$\nu_{\text{as}}(\text{ND}_2)$	2654 (w)	2660	2658 (5)	2668 (6)	2612 (4)	2614 (3)
$\nu_{\text{s}}(\text{ND}_2)$	2512 (w)		2518 (4)	2524 (6)	2488 (5)	2488 (4)
$\nu(\text{ND})$	2512 (w)		2515 (5)	2512 (5)	2507 (5)	2511 (4)
$\nu(\text{C}=\text{N})$	1662 (s)	1662	1647 (100)	1650 (100)	1677 (100)	1667 (100)
$\nu(\text{C}-\text{N}) + \nu(\text{C}-\text{O})$	1393 (m)		1367 (53)	1359 (49)	1317 (71)	1306 (71)
$\delta(\text{ND}_2)$			1179 (1)	1156 (3)	1168 (6)	1184 (1)
$\delta(\text{OD})$	1017 (w)		1014 (8)	990 (13)	966 (2)	969 (13)
$\rho(\text{ND}_2) + \rho(\text{ND})$			892 (15)	883 (5)	922 (11)	898 (2)
$\nu(\text{C}-\text{N}) + \nu(\text{C}-\text{O})$			848 (<1)	840 (0)	875 (3)	854 (8)
$\rho(\text{ND}_2) + \rho(\text{ND})$	814 (w)		801 (6)	807 (19)	809 (14)	827 (9)
$\omega(\text{CNO})$	723 (w)		710 (6)	709 (6)	684 (10)	677 (15)
$\tau(\text{ND})$			554 (5)	526 (6)	619 (3)	575 (10)
$\delta(\text{CNO})$			478 (8)	473 (5)	475 (20)	508 (3)
$\delta(\text{CNO})$			420 (<1)	435 (0)	467 (18)	461 (20)
$\tau(\text{OD})$			382 (5)	312 (5)	421 (2)	423 (3)
$\omega(\text{ND}_2)$			355 (34)	369 (34)	290 (19)	282 (16)
$\tau(\text{ND}_2)$			241 (5)	210 (5)	272 (5)	247 (4)
$E_{\text{relative}}$ (kJ/mol)			0	8.5	14	31

<sup>a</sup> Intensity of signal: s, strong; m, medium; and w, weak. <sup>b</sup> Calculated frequencies are scaled by a standard factor of 0.97. Normalized IR intensities are given in parentheses. <sup>c</sup>  $\nu$ , stretching;  $\delta$ , bending;  $\rho$ , rocking;  $\tau$ , torsion; and  $\omega$ , wagging.

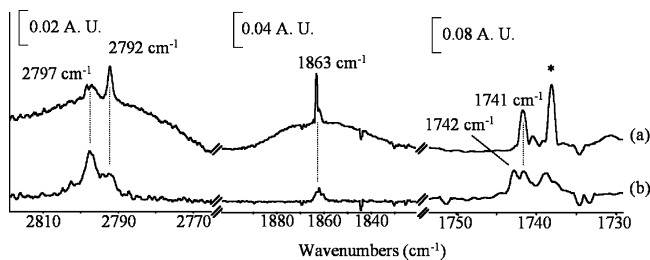


**Figure 6.** Comparison between the FTIR spectrum of irradiated urea ( $\lambda > 160$  nm, 450 min, annealing at 10 K) in argon (spectrum a) with the FTIR spectrum of a similar irradiated CO/N<sub>2</sub>H<sub>4</sub>/Ar 1/4/900 mixture (spectrum b). The residual urea band is marked with an asterisk (“\*”).

To recognize the origin of these bands, we have, in turn, irradiated (in a similar manner to that previously described) the HNCO:NH<sub>3</sub> and CO:N<sub>2</sub>H<sub>4</sub> complexes in argon matrixes. Within a similar irradiation time to that necessary for the destruction of urea (ca. 450 min), we did not observe any reductions in intensity for absorption bands assigned to the HNCO:NH<sub>3</sub> complex in argon. We can thus conclude that this complex is stable under VUV irradiation ( $\lambda > 160$  nm). Consequently, a plateau is observed for high irradiation times in the kinetic curve of HNCO:NH<sub>3</sub> in argon (see Figure 4).

As observed in Figure 4, the behavior of the CO:N<sub>2</sub>H<sub>4</sub> complex is different from that of the HNCO:NH<sub>3</sub> complex, mainly for irradiation times in excess of 300 min (argon matrix), which were sufficient to produce a slight reduction in the CO:N<sub>2</sub>H<sub>4</sub> absorptions. The comparison between spectra recorded after the irradiation of the CO/N<sub>2</sub>H<sub>4</sub> mixture in argon ( $\lambda > 160$  nm) to that obtained after the urea irradiation reveals similar absorptions at 2797, 2792, 1742, and 1741 cm<sup>-1</sup> (Figure 6). These frequencies are consistent with formaldehyde (H<sub>2</sub>CO) absorptions,<sup>41</sup> which displays in its monomeric form an intense peak at 2797 cm<sup>-1</sup> and a weaker peak at 1742 cm<sup>-1</sup>. Thus, the position of these four peaks suggests that H<sub>2</sub>CO is present under two forms in the mixture: the monomeric form (2797 and 1742 cm<sup>-1</sup>) and a complexed form (2792 and 1741 cm<sup>-1</sup>). This latter form can be tentatively assigned to the H<sub>2</sub>CO:N<sub>2</sub>H<sub>2</sub> complex. In addition, a weak band at 1315 cm<sup>-1</sup>, observed during the CO/N<sub>2</sub>H<sub>4</sub>/Ar mixture photolysis, can be assigned to a vibrational mode of N<sub>2</sub>H<sub>2</sub>.<sup>42</sup>

The evolution of isourea bands during irradiation (see Figure 4) supports the concept that this compound acts as an intermediate species in the involved photochemical process. The presence of additional spectral features, as yet not assigned, in the water absorption regions (3718 and 1598 cm<sup>-1</sup>) may indicate the formation of a new molecular complex that contains H<sub>2</sub>O. It follows, according to urea stoichiometry, that H<sub>2</sub>O, along with NH<sub>2</sub>CN or HNCNH, would be formed from isourea in the dehydration process(es).

**4.7. Formation of NH<sub>2</sub>CN:H<sub>2</sub>O Complex.** To identify and verify the nature of this complex, we have compared the spectra obtained at 10 K of co-deposited NH<sub>2</sub>CN/Ar and H<sub>2</sub>O/Ar mixtures (Figure 7b) with the spectrum resulting from urea-h<sub>4</sub> irradiation (see Figure 7a). In the typical region of the  $\nu(\text{OH})$  stretching mode (3800–3680 cm<sup>-1</sup>), the NH<sub>2</sub>CN/H<sub>2</sub>O/Ar mixture shows a new absorption band at 3718 cm<sup>-1</sup> in the vicinity of the rotational band of the  $\nu_3$  mode of water<sup>43</sup> located at 3739 cm<sup>-1</sup>. In the OH bending region (1610–1560 cm<sup>-1</sup>), we observe a band at 1598 cm<sup>-1</sup>, which is absent in the infrared spectra of monomer species (see Figure 7c, 7d). Finally, in the region related to the cyanamide most-intense mode ( $\nu(\text{CN})$ ) (2290–2210 cm<sup>-1</sup>),<sup>20</sup> we observe a new band at 2258 cm<sup>-1</sup>, slightly downshifted from the monomer frequency ( $\Delta\nu = -6$  cm<sup>-1</sup>). These new bands also appear in the spectrum of irradiated urea-h<sub>4</sub> (see Figure 7a, Table 2). This confirms the formation of a cyanamide/water complex during the photolysis. Several theoretical studies on the hydration of cyanamide have already been performed.<sup>44,45</sup> They show that the interaction between cyanamide and water molecules (a 1:1 complex) can be described in terms of hydrogen-bond formation (H<sub>2</sub>O⋯H<sub>2</sub>CN).

Similarly, by the comparison of the irradiated urea-d<sub>4</sub> spectrum (Figure 8a) with the spectrum of ND<sub>2</sub>CN/Ar and D<sub>2</sub>O/Ar co-deposited mixtures (see Figure 8b), we assign several bands to the ND<sub>2</sub>CN:D<sub>2</sub>O complex. These are listed with their assignments in Table 3 and are located at 2761, 2258, and 1180 cm<sup>-1</sup>. The most striking feature in the  $\nu(\text{C}=\text{N})$  region is the intense absorption at 2109 cm<sup>-1</sup> (see Figure 8a). This value is close to the  $\nu(\text{NCN})$  antisymmetric stretching mode frequency of carbodiimide (DNCND), which is reported in the literature to be the most intense IR feature, located at 2107 cm<sup>-1</sup>.<sup>20</sup> It is



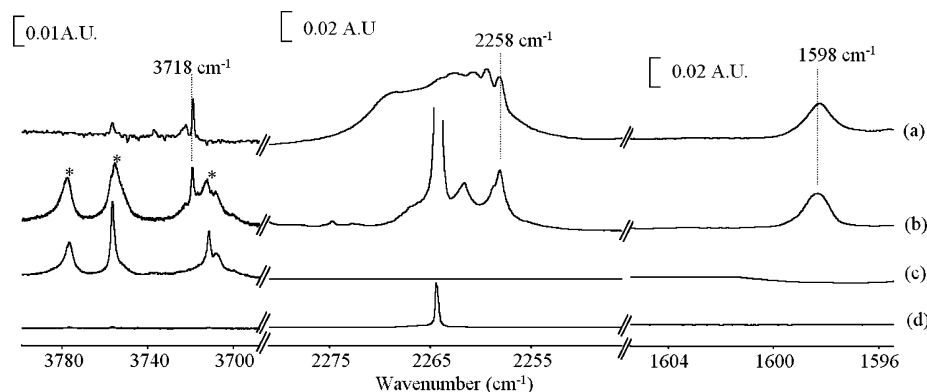


**Figure 7.** Comparison between the FTIR spectra (argon matrixes, 10 K) of urea, VUV-irradiated for 450 min (spectrum a),  $\text{NH}_2\text{CN}/\text{H}_2\text{O}$  mixture (spectrum b),  $\text{H}_2\text{O}$  ( $\text{H}_2\text{O}/\text{Ar}$  ratio 10/250) (spectrum c), and cyanamide (spectrum d). The rotational band of water is marked with an asterisk (“\*”). Dotted lines label the  $\text{NH}_2\text{CN}:\text{H}_2\text{O}$  complex.

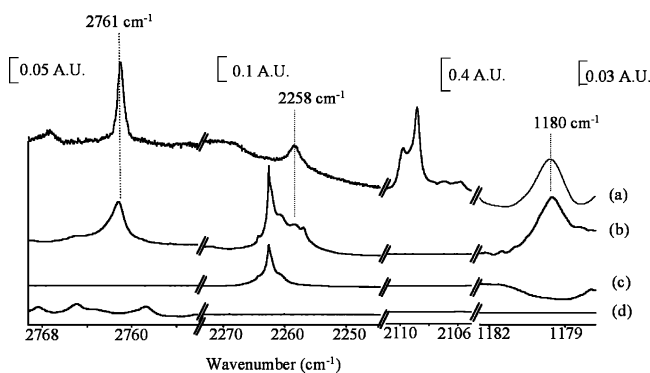


**Figure 8.** Comparison between the FTIR spectra (argon matrixes, 10 K) of urea- $d_4$ , VUV-irradiated for 450 min (spectrum a);  $\text{ND}_2\text{CN}/\text{D}_2\text{O}$  mixture (spectrum b);  $\text{D}_2\text{O}$  ( $\text{D}_2\text{O}/\text{Ar}$  ratio = 10/250) (spectrum c), and cyanamide- $d_2$  (spectrum a). Dotted lines label the  $\text{ND}_2\text{CN}:\text{D}_2\text{O}$  complex.

also interesting to note that, during the photolysis of urea- $h_4$ , we did not observe the analogous band in this region.

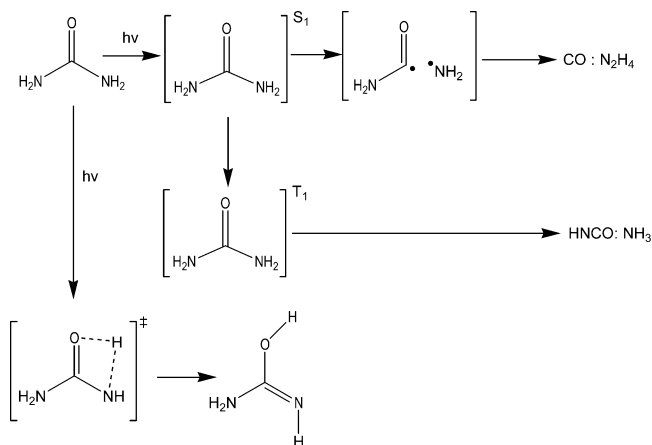
In the xenon matrix, three bands appeared after the photolysis of urea- $h_4$  (urea- $d_4$ ), at 3700, 2257, and 1588  $\text{cm}^{-1}$  (2747, 2258, and 1182  $\text{cm}^{-1}$ ), which we assign to the  $\text{NH}_2\text{CN}:\text{H}_2\text{O}$  complex (see Tables 2 and 3); these frequencies are similar to those obtained in argon at 3718, 2258, and 1598  $\text{cm}^{-1}$  (2761, 2258, and 1180  $\text{cm}^{-1}$ ). As previously, the band located at 3700  $\text{cm}^{-1}$  is assigned to the  $\nu(\text{OH})$  stretching mode of water downshifted in frequency by the interaction with cyanamide, whereas the bands at 1588 and 2257  $\text{cm}^{-1}$  are due to the  $\delta(\text{OH})$  and  $\nu(\text{CN})$  modes of cyanamide in the  $\text{H}_2\text{O}:\text{NH}_2\text{CN}$  complex.

## 5. Discussion

The VUV irradiation ( $\lambda > 160$  nm) of urea- $h_4$  (urea- $d_4$ ) leads to the formation of new species coming from three different reaction pathways. These products include  $\text{CO}:\text{N}_2\text{H}_4$  ( $\text{CO}:\text{N}_2\text{D}_4$ ) and  $\text{HNCO}:\text{NH}_3$  ( $\text{DNCO}:\text{ND}_3$ ) molecular complexes, and the isourea molecule  $\text{NH}_2(\text{HO})\text{C}=\text{NH}$  ( $\text{ND}_2(\text{DO})\text{C}=\text{ND}$ ). Scheme 1 gives a mechanistic view, indicating the routes toward new species. Given the molecular complexes that were formed, it seems rational to presume that the crucial step in their formation consists of the cleavage of the urea C–N bond. The occurrence of this photochemical process ( $\alpha$ -cleavage) is well-known for aromatic and aliphatic amides.<sup>11,12,46</sup> In the present case, it should lead to the radical pair  $\text{NH}_2\text{CO} + \text{NH}_2$ .

It is interesting to compare the urea photochemistry to that of formamide. In the argon matrix, Lundell et al.<sup>9</sup> demonstrated that the photodecomposition of formamide with a 193-nm excimer laser radiations leads to a molecular complex  $\text{CO}:\text{NH}_3$

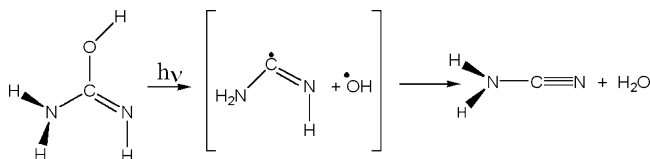
## SCHEME 1: Possible Mechanism for Production of $\text{CO}$ and $\text{N}_2\text{H}_4$ , $\text{HNCO}$ , and $\text{NH}_3$ or Isourea



(which exists under two different forms:  $\text{NH}_3\text{--CO}$  and  $\text{NH}_3\text{--OC}$ ) and the  $\text{HNCO}:\text{H}_2$  complex.<sup>9,47</sup> From a theoretical point of view, formamide photoexcited to its  $S_1$  state can deactivate via two radiationless pathways: (i) dissociation into  $\text{NH}_2$  and  $\text{CHO}$  radicals within the  $S_1$  surface, finally leading to  $\text{CO}$  and  $\text{NH}_3$ , and (ii) intersystem crossing to the  $T_1$  surface, via a  $S_1/T_1$  crossing point, to form  $\text{HNCO}:\text{H}_2$ .<sup>11</sup>

Photons available in the present experiment ( $E < 750$  kJ/mol) were sufficiently energetic to excite the urea molecule to its first excited singlet state  $S_1$ . The  $\alpha$ -cleavage operative within the  $S_1$  potential energy surface then would yield  $\text{NH}_2\text{CO}$  and  $\text{NH}_2$ . However, no radical is observable, indicating that radicals evolve very quickly in the matrix cage to rearrange into new species. The  $\text{NH}_2\text{CO}$  radical is dissociated into  $\text{NH}_2 + \text{CO}$ , and then the recombination of two  $\text{NH}_2$  radicals yields the complex  $\text{CO}:\text{N}_2\text{H}_4$ , which is the final product of the decarbonylation process.

The choice of the host gas for the matrix is also very important, because of its influence on the mechanism of urea photodissociation. It is well-known that the intersystem crossing between  $S_1$  and  $T_1$  states is accelerated by heavy atoms. Numerous examples of the “external heavy atom” effect induced by Xe are available in the literature.<sup>48,49</sup> As noted previously, the  $\text{HNCO}:\text{NH}_3$  complex is the major product in the xenon matrix, whereas the  $\text{CO}:\text{N}_2\text{H}_4$  complex also is obtained but in trace amounts. Thus, in xenon, crossing between urea  $S_1$  and  $T_1$  potential energy surfaces is likely to generate the  $\text{HNCO}:\text{NH}_3$  complex from this latter surface. In a very similar manner, as recognized by Lundell et al., the formamide irradiation in xenon increased the yield of  $\text{HNCO}:\text{H}_2$  formation.<sup>9</sup>

**SCHEME 2: Possible Mechanism for the Production of Cyanamide (NH<sub>2</sub>CN) and H<sub>2</sub>O from Isoourea**


The isourea (NH<sub>2</sub>(HO)C=NH) is observed as well in argon matrixes as in xenon matrixes. In argon, the most-stable isourea stereoisomer, with the (s-Z)-(E) configuration, is formed. The stereochemistry of this compound is similar to that observed during the formamide irradiation (248 nm), which led to formimidic acid H(HO)C=NH in its most-stable form.<sup>39</sup> The electronic state engaged in this transformation of formamide is S<sub>1</sub>, of the n-π\* character (220 nm), which is less energetic than S<sub>2</sub>, of the π-π\* character (169 nm). For urea, both n-π\* (178 nm) and π-π\* (161 nm) transitions are relatively similar in energy and we cannot conclude from which state (S<sub>1</sub> or S<sub>2</sub>) the isourea originates. The isourea should be created following an intramolecular 1,3 H shift, which probably involves a four-centered transition state, as it was shown by the ab initio calculations for the similar cases of formamide and acetamide.<sup>11,12</sup> Isoourea is detected in a very small amount during all the VUV process, because it is present only as an intermediate (see Figure 4), which eventually, although a dehydration process, leads to products such as the NH<sub>2</sub>CN:H<sub>2</sub>O complex. Indeed, the formation of cyanamide (NH<sub>2</sub>CN) from urea involves a C-O bond cleavage, which occurs more easily in the case of isourea (single bond) than for urea (double bond). The C-O bond cleavage of isourea would lead to the radical pair [NH<sub>2</sub>CNH + OH] in the Ar cage, whereas, in the following step, NH<sub>2</sub>CN and H<sub>2</sub>O should be produced by hydrogen transfer from NH<sub>2</sub>CNH to a OH radical (Scheme 2). This latter radical has been detected by laser-induced fluorescence during the photochemical decomposition of formaldoxime [CH<sub>2</sub>NOH], which is a formimidic acid isomer.<sup>53</sup> Formaldoxime leads to the HCN:H<sub>2</sub>O or HNC:H<sub>2</sub>O complexes.<sup>53</sup> The formation of CH<sub>3</sub>CN and H<sub>2</sub>O, but not of the CH<sub>3</sub>C(OH)=NH intermediate, has been reported in the experimental study on acetamide photolysis. Therefore, the detection of isourea (H<sub>2</sub>NC(OH)=NH) gives new insight into the photochemistry of carboxamides.

In the same way, we suppose isourea-d<sub>4</sub> to be the precursor of the D<sub>2</sub>NCN:D<sub>2</sub>O complex. Moreover, during the UV irradiation of urea-d<sub>4</sub>, we noticed the presence of a vibrational band located at 2109 cm<sup>-1</sup>, which is in good agreement with the most intense absorption expected for carbodiimide-d<sub>2</sub> (DNCND).<sup>20</sup> As described in a previous work, the formation of this molecule should result from a photoisomerization reaction that converts cyanamide into carbodiimide at λ > 160 nm.<sup>54,55</sup> However, we did not detect the formation of carbodiimide-h<sub>2</sub> during the irradiation of urea-h<sub>4</sub>, with the probable reason being the kinetic isotopic effect.

We also investigated the secondary species issued from the photodegradation of primary products. For the HNCO:NH<sub>3</sub> complex, we found this system to be stable when irradiated in the λ > 160 nm range. It should be underlined that uncomplexed matrix-isolated NH<sub>3</sub> is known to undergo dissociation at λ > 170 nm.<sup>50</sup> The complexation-induced stability of ammonia has also been reported for the CO:NH<sub>3</sub> complex and can be explained by the absorption of energy by CO molecule, with which NH<sub>3</sub> interacts.

For the CO:N<sub>2</sub>H<sub>4</sub> complex, a slight decrease of its vibrational bands is observed after >300 min of irradiation, in an argon

matrix, where it is produced in a relatively higher amount than in xenon. This decrease is due to N<sub>2</sub>H<sub>4</sub>, which has a broad absorption spectrum between 150 nm and 230 nm.<sup>51</sup> In the gas phase, the major decomposition channel leads to H + N<sub>2</sub>H<sub>3</sub>.<sup>52</sup> Thus, the primary excitation of CO:N<sub>2</sub>H<sub>4</sub> complex in solid argon presumably produces a radical pair [HCO + N<sub>2</sub>H<sub>3</sub>] in the matrix cage, from which H<sub>2</sub>CO and N<sub>2</sub>H<sub>2</sub> may originate as secondary products. Several weak absorption bands (see Table 2) are observed to be in good agreement with the aforementioned species. A small absorption band observed at 1863 cm<sup>-1</sup> is consistent with the presence of the HCO radical.<sup>56</sup>

**6. Conclusion**

Vacuum ultraviolet (VUV) irradiation (wavelength of λ > 160 nm) of urea-h<sub>4</sub> and urea-d<sub>4</sub> isotopomer in argon at 10 K leads to the formation of molecular complexes HNCO:NH<sub>3</sub>, CO:N<sub>2</sub>H<sub>4</sub>, and their deuterated analogues. The characterization of complexes was possible after separate depositions of respective pairs of compounds in argon matrixes. These complexes have the stoichiometry of the urea precursor, which shows that the cage effect inhibits the exit of primary photolysis products. Isoourea, which is detected for the first time, results from the photoisomerization of urea. With the support of theoretical calculations, we demonstrated that isourea-h<sub>4</sub> (isourea-d<sub>4</sub>) is isolated in the matrix in its (s-Z)-(E) configuration. This tautomer has an intermediate role in the ultraviolet (UV) process, leading, by dehydration, to the secondary product, the molecular complex NH<sub>2</sub>CN:H<sub>2</sub>O (ND<sub>2</sub>CN:D<sub>2</sub>O). Ultimately, we observed that only the deuterated form of the latter can be converted to the DNCND:D<sub>2</sub>O complex.

In the xenon matrix, the photodecomposition of urea is different, because of the external heavy atom effect induced by the host medium on the initially formed radical pair. This effect increases the rate of the intersystem crossing from an excited singlet state to a triplet state, leading to the production of the HNCO:NH<sub>3</sub> complex as the primary product. Finally, the CO:N<sub>2</sub>H<sub>4</sub> (CO:N<sub>2</sub>D<sub>4</sub>) complex is determined to be dissociated to H<sub>2</sub>CO and probably N<sub>2</sub>H<sub>2</sub> (D<sub>2</sub>CO and N<sub>2</sub>D<sub>2</sub>). However, based on our experimental results, ab initio theoretical study of the ground and excited states is necessary to hone the reaction pathways for urea decomposition.

Based on these results, which have been obtained in cryogenic rare gas matrixes, we plan an analogous study of urea trapped in water ice, which has direct relevance to astrochemical issues.

**Acknowledgment.** The “Programme National de Physique et Chimie du Milieu Interstellaire” is gratefully acknowledged for the financial support of this work. We are very grateful to Pr. R. Kolos for “fruitful discussions”.

**Supporting Information Available:** The MP2/6-311+(2d,2p) calculated frequencies of the four conformers of the isourea-h<sub>4</sub> and isourea-d<sub>4</sub> (Tables 1S and 2S). (PDF.) This material is available free of charge via the Internet at <http://pubs.acs.org>.

**References and Notes**

- (1) Wöhler, F. *Ann. Phys. Chem.* **1828**, *12*, 253.
- (2) Lohrman, R.; Orgel, L. E. *Science* **1971**, *117*, 528.
- (3) Terasaki, M.; Nomoto, S.; Mita, H.; Shimoyama, A. *Origins Life Evol. Biosphere* **2002**, *32*, 91.
- (4) Robertson, M. P.; Miller, S. L. *Nature* **1995**, *375*, 772.
- (5) Raunier, S.; Chiavassa, T.; Duvernay, F.; Borget, F.; Aycard, J. P.; Dartois, E.; D'Hendecourt, L. *Astron. Astrophys.* **2004**, *416*, 165.
- (6) Hartquist, T. W.; Williams, D. A. *The Chemically Controlled Cosmos*; Cambridge University Press: New York, 1995.

- (7) Back, R. A.; Boden, J. C. *Trans. Faraday Soc.* **1971**, *69*, 88.
- (8) Kakumoto, T.; Saito, K.; Imamura, A. *J. Phys. Chem.* **1985**, *89*, 2286.
- (9) Lundell, J.; Krajewska, M.; Räsänen, M. *J. Phys. Chem. A* **1998**, *102*, 6643.
- (10) Bosco, S. R.; Cirillo, A.; Timmons, R. B. *J. Am. Chem. Soc.* **1969**, *91*, 3140.
- (11) Liu, D.; Fang, W. H.; Fu, X. *Chem. Phys. Lett.* **2000**, *318*, 291.
- (12) Chen, X. B.; Fang, W. H.; Fang, D. C. *J. Am. Chem. Soc.* **2003**, *125*, 9689.
- (13) Campbell, B. F.; Clark, L. B. *J. Am. Chem. Soc.* **1989**, *111*, 8131.
- (14) Elbert, S. T.; Davidson, E. R. *Int. J. Quantum Chem.* **1974**, *8*, 857.
- (15) Sánchez de Merás, A. M. J.; Cuesta, I. G.; Kosh, H. *Chem. Phys. Lett.* **2001**, *348*, 469.
- (16) Herzberg, G.; Reid, C. *Discuss. Faraday Soc.* **1950**, *9*, 92.
- (17) Sheludiyakov, Y. L.; Shubareva, F. Z.; Golodov, V. A. *J. Appl. Chem.* **1994**, *67*, 780.
- (18) Jacox, M. E.; Milligan, D. E. *J. Chem. Phys.* **1964**, *40*, 2457.
- (19) Kubulat, K.; Person, W. B. *J. Phys. Chem.* **1989**, *93*, 2917.
- (20) King, S. T.; Strobe, J. H. *J. Chem. Phys.* **1971**, *54*, 1289.
- (21) Frisch, M. J.; Trucks, G. W.; Schlegel, H. B.; Scuseria, G. E.; Robb, M. A.; Cheeseman, J. R.; Zakrzewski, V. G.; Montgomery, J. A., Jr.; Stratmann, R. E.; Burant, J. C.; Dapprich, S.; Millam, J. M.; Daniels, A. D.; Kudin, K. N.; Strain, M. C.; Farkas, O.; Tomasi, J.; Barone, V.; Cossi, M.; Cammi, R.; Mennucci, B.; Pomelli, C.; Adamo, C.; Clifford, S.; Ochterski, J.; Petersson, G. A.; Ayala, P. Y.; Cui, Q.; Morokuma, K.; Malick, D. K.; Rabuck, A. D.; Raghavachari, K.; Foresman, J. B.; Cioslowski, J.; Ortiz, J. V.; Stefanov, B. B.; Liu, G.; Liashenko, A.; Piskorz, P.; Komaromi, I.; Gomperts, R.; Martin, R. L.; Fox, D. J.; Keith, T.; Al-Laham, M. A.; Peng, C. Y.; Nanayakkara, A.; Gonzalez, C.; Challacombe, M.; Gill, P. M. W.; Johnson, B. G.; Chen, W.; Wong, M. W.; Andres, J. L.; Head-Gordon, M.; Replogle, E. S.; Pople, J. A. *Gaussian 98*, revision A.7; Gaussian, Inc.: Pittsburgh, PA, 1998.
- (22) Lee, C.; Yang, W.; Parr, R. *Phys. Rev. B* **1988**, *37*, 785.
- (23) Boys, S.; Bernardy, F. *Mol. Phys.* **1970**, *19*, 553.
- (24) Godfrey, P. D.; Brown, R. D.; Hunter, A. N. *J. Mol. Struct.* **1997**, *413*, 405.
- (25) King, S. *Spectrochim. Acta, Part A* **1972**, *28A*, 165.
- (26) Li, X.; Stotesbury, S. J.; Jayasooriya, U. A. *Spectrochim. Acta, Part A* **1987**, *43A*, 1595.
- (27) Worsham, J. E.; Levry, H. A.; Peterson, S. W. *Acta Crystallogr.* **1957**, *10*, 319.
- (28) Swaminathan, B. M.; Carven, R. K.; McMullan, R. K. *Acta Crystallogr., Sect. B: Struct. Sci.* **1984**, *B40*, 300.
- (29) Guth, H.; Heger, G.; Klein, S.; Treutmann, W.; Scheringer, C. Z. *Kristallogr.* **1980**, *153*, 237.
- (30) Miao, M. S.; Keuleers, R.; Desseyn, H. O.; Van Alsenoy, C.; Martins, J. L. *Chem. Phys. Lett.* **2000**, *316*, 297.
- (31) Rousseau, B.; Van Alsenoy, C.; Keuleers, R.; Desseyn, H. O. *J. Phys. Chem. A* **1998**, *102*, 6540.
- (32) Dobrowolski, J. Cz.; Kolos, R.; Sadlej, J.; Mazurek, A. P. *Vib. Spectrosc.* **2002**, *29*, 261.
- (33) Raunier, S.; Chiavassa, T.; Marinelli, F.; Allouche, A.; Aycard, J. P. *J. Phys. Chem. A* **2003**, *107*, 9335.
- (34) Duvernay, F.; Hirota, N.; Shinohara, H.; Nishi, N. *J. Phys. Chem.* **1985**, *89*, 2260.
- (35) Teles, J. H.; Maier, G.; Hess, B. A., Jr.; Schaad, L. J.; Winnewisser, M.; Winnewisser, B. P. *Chem. Ber.* **1989**, *122*, 753.
- (36) Duvernay, F.; Chiavassa, T.; Borget, F.; Aycard, J. P. *Chem. Phys.* **2004**, *298*, 241.
- (37) Tipton, T.; Stone, D. A.; Kubulat, K.; Person, W. B. *J. Phys. Chem.* **1989**, *93*, 2917.
- (38) Dubost, H.; Abouaf-Marguin, L. *Chem. Phys. Lett.* **1972**, *17*, 269.
- (39) Maier, G.; Endres, J. *Eur. J. Org. Chem.* **2000**, 1061.
- (40) Piasek, Z.; Urbanski, T. *Tetrahedron Lett.* **1962**, *16*, 723.
- (41) Khoshkhoo, H.; Nixon, E. R. *Spectrochim. Acta, Part A* **1973**, *29A*, 603.
- (42) Minkwitz, R. *Anorg. Allg. Chem.* **1975**, *411*, 1.
- (43) Ayers, G. P.; Pulling, D. E. *Spectrochim. Acta, Part A* **1976**, *32A*, 1629.
- (44) Tordini, F.; Bencini, A.; Bruschi, M.; De Gioia, L.; Zampella, G.; Fantucci, P. *J. Phys. Chem. A* **2003**, *107*, 1188.
- (45) Lewis, M.; Glaser, R. *J. Am. Chem. Soc.* **1998**, *120*, 8541.
- (46) Klessinger, M.; Michl, J. *Excited States and Photochemistry of Organic Molecules*; VCH: New York, 1995.
- (47) Lundell, J.; Krajewska, M.; Räsänen, M. *J. Mol. Struct.* **1998**, *448*, 221.
- (48) Kunttu, H.; Dahlqvist, M.; Murto, J.; Räsänen, M. *J. Phys. Chem.* **1988**, *92*, 1495.
- (49) Lundell, J.; Räsänen, M. *J. Mol. Struct.* **1997**, *436*, 349.
- (50) Okabe, H. *Photochemistry of Small Molecules*; Wiley-Interscience: New York, 1978.
- (51) Syage, J. A.; Cohen, R. B.; Steadman, J. J. *Chem. Phys.* **1992**, *97*, 6072.
- (52) Hawkins, W. G.; Houston, P. L. *J. Phys. Chem.* **1984**, *86*, 704.
- (53) Heikkilä, A.; Pettersson, M.; Lundell, J.; Kriachtchev, L.; Räsänen, M. *J. Phys. Chem. A* **1999**, *103*, 2945.
- (54) Maier, G.; Eckert, J.; Bothur, A.; Reisenauer, H. P.; Schimdt, C. *Liebigs Ann.* **1996**, 1041.
- (55) Duvernay, F.; Chiavassa, T.; Borget, F.; Aycard, J. P. *J. Phys. Chem. A* **2005**, *109*, 603.
- (56) Milligan, D. E.; Jacox, M. E. *J. Chem. Phys.* **1969**, *51*, 277.